

# We are IntechOpen, the world's leading publisher of Open Access books Built by scientists, for scientists

4,200

Open access books available

116,000

International authors and editors

125M

Downloads

Our authors are among the

154

Countries delivered to

TOP 1%

most cited scientists

12.2%

Contributors from top 500 universities



WEB OF SCIENCE™

Selection of our books indexed in the Book Citation Index  
in Web of Science™ Core Collection (BKCI)

Interested in publishing with us?  
Contact [book.department@intechopen.com](mailto:book.department@intechopen.com)

Numbers displayed above are based on latest data collected.  
For more information visit [www.intechopen.com](http://www.intechopen.com)



---

# Application of Optical Methods to Electronic Component Stress Analysis

---

Caterina Casavola, Luciano Lamberti,  
Vincenzo Moramarco, Giovanni Pappalettera and  
Carmine Pappalettere

Additional information is available at the end of the chapter

<http://dx.doi.org/10.5772/intechopen.82714>

---

## Abstract

Increasing electronic component reliability is, nowadays, a hot topic both in most advanced applications as well as in electronic devices of common use in everyday life. In fact, requirements in terms of miniaturization of electronics components introduce issues connected with heat dissipation management. Materials, packaging, heat dissipator, and even positioning of the component on the board should be optimized in order to reduce thermal stresses generated in the components, which are one of the most important failure mechanisms of electronics. Thermal stress evaluation is, however, a difficult task due to the size of the elements under testing and to the necessity of measuring small amount of strains. At the same time, any contact with the object under measurement should be avoided not to alter heat capacity of the component itself. In this work, some results of experimental stress analysis gathered using electronic speckle pattern interferometry will be described; it will be pointed out how this approach allows to put in evidence inhomogeneous stress fields undergone by the electronic components and how it is possible to highlight the presence of bad functioning and defects.

**Keywords:** electronic component reliability, electronic speckle pattern interferometry, bad thermal contact, deformation field, damage detection

---

## 1. Introduction

Electronic components are, nowadays, widely spread at any level from simple personal devices to very demanding equipment for aerospace applications. Independently of their specificity,

it is a general rule that they are subjected to thermal loading as a consequence of the Joule effect connected to the running electric current. This introduces a mechanical problem because thermal deformations can determine crack initiation and propagation [1, 2]. In this view, the possibility to have accurate and detailed information on the mechanical behavior of the component during working is important. However, due to the complexity of electronic components [3], experimental methods are strictly necessary. Different experimental approaches have been used to the scope such as acoustic microscopy, X-ray, and thermography [4, 5]. Among these, X-ray and infrared thermography are the most common ones. The use of optical methods has also been explored by several authors [6–9]. These methods rely on the modulation in the reflected/diffused light wavefront connected with deformation of the surface. Demodulation of the information allows us to determine displacement field. Interestingly, this can be done without any contact with the component. From the above-mentioned survey, it appears that speckle and moiré are the OT most commonly used in the analysis of electronic chips. Speckle and moiré methods, in particular, have been applied several times in the analysis of electronic chips. In particular, the phase shifting electronic speckle pattern interferometry (PS-ESPI) is very appealing because it does not require application of a grating and can guarantee very high sensitivity [10]. As it was previously underlined, localized mechanical damage can lead to stress/strain concentration that can cause component rupture. If cyclic loading is considered, this mechanism can also be driven by progressive damage accumulation. Moreover, it should be taken into account that the presence of a damage can alter the electrical resistance. This also alters thermal distribution. Proper mounting of the components is a determinant stage in thermal management. In fact, inappropriate mounting can introduce bad thermal contact, which alters thermal dissipation capability of the chip. In this chapter, the PSESPI technique will be applied to analyze displacement fields of components under different conditions. It will be applied on a Darlington transistor (NKT605) to evaluate its mechanical response when powered. The same will also be studied under anomalous loading conditions to understand which kind of effects this introduces on the mechanical behavior. Furthermore, the components will be analyzed when subjected to successive powering cycles in order to understand if deformation of the component is completely recovered at the end of the cycle or some plastic deformations remain. Finally, a voltage stabilizer will be studied; in this case, two different conditions of thermal contact will be analyzed to understand if it is possible, by analyzing the displacement fields, to distinguish between those two conditions. It should finally underline that, in addition to the specific case studies and applications that will be discussed in this chapter, authors intend to put in evidence a more general aspect, which is overall connected to the potentiality and the versatility of an approach based on optical methods. As there is no contact with the measured specimen, optical methods can be used even if the component is highly miniaturized without altering heat dissipation of the component itself. In addition, this can be done independently of the complexity of the analyzed component that can be very high as for the case of ASIC and FPGA components. Finally, it should be pointed out that spatial resolution of this technique is basically connected with resolution of the employed camera. Nowadays, technological developments allow to easily get high resolution camera at low price, so that it is easy to reach micrometric resolution. Hence, dedicate analysis in a critical region or in correspondence of a pad to detect malfunctioning, bad thermal contact, and hot point can be done at a resolution not achievable by thermographic methods. Feasibility of

use of the proposed approach to the analysis of other types of chips (e.g., ASIC or FPGA with ball grid arrays) is briefly discussed at the end of the chapter.

## 2. Materials and methods

The system that was built up to measure the displacement field on the Darlington transistor and the positive voltage stabilizer following the general plan reported in the Introduction section is based on the electronic speckle pattern interferometry. In this specific optical technique, the information is carried out by the random light distribution which is obtained whenever a coherent beam of light illuminates a rough surface. If the illuminated surface is deformed, speckle pattern also changes as a consequence. Here, a double illumination interferometer [11] was built up, which is sensitive to the in-plane horizontal displacement component. **Figure 1** shows the schematic of the experimental set-up utilized in this research.

The setup included a 17 mW He-Ne laser beam ( $\lambda = 632.8$  nm), which goes through a spatial filter, and it is collimated before illuminating the surface. An intensity beam splitter is used to divide the beam into two paths. The emerging beams are reflected by mirrors M2 and M3 and then directed at the same angle toward the surface. In this way, symmetric double illumination is obtained. A black and white Marlin FireWire Allied Vision Technologies camera was used to capture images whose sensor has  $1628 \times 1236$  pixel. Camera was equipped with imaging lenses with field-of-view = 21 mm. The optical axis of the camera is perpendicular to the component under analysis. Temporal phase shifting approach [13] was utilized in order to recover phase of the speckle correlation fringes. For that purpose, a piezoelectric translator is inserted into one of the arms of the interferometer in order to allow phase shifting. In particular, the five-step technique was adopted in which subsequent  $\pi/2$  shifts are introduced, so that the following sequence is generated:  $\varphi_n = 0, \pi/2, \pi, 3\pi/2, 2\pi$  ( $n = 1, \dots, 5$ ). It should be noted that the phase of the first and last image is the same. The following expression can be used to obtain the phase difference encoded in the speckle correlation fringes:

$$\Delta\varphi(x, y) = \tan^{-1} \frac{2I_2(x, y) - I_4(x, y)}{2I_3(x, y) - I_5(x, y) - I_1(x, y)} \quad (1)$$

where  $I_1(x, y)$ ,  $I_2(x, y)$ ,  $I_3(x, y)$ ,  $I_4(x, y)$  and  $I_5(x, y)$  are light intensity values of the correlation fringe patterns generated for each phase shift. In order to improve the data quality, it was decided to preprocess fringes before extracting phase information. After some preliminary investigation, it was decided to apply a median filter to the image. This filter replaces, for each pixel, the median value calculated over the neighborhood pixels. A  $7 \times 7$  pixel window was adopted for these specific measurements. With the same aim of improving data quality, it was decided to apply a white sprayed layer to the inspected components. This was done to improve fringe contrast in order to have benefits in terms of final accuracy. The in-plane displacement components  $u$  of each generic point  $P(x, y)$  of the specimen can be obtained by the following expression:

$$u(x, y) = \frac{\Delta\varphi(x, y)}{2\pi} \cdot \frac{\lambda}{2 \sin \vartheta} \quad (2)$$

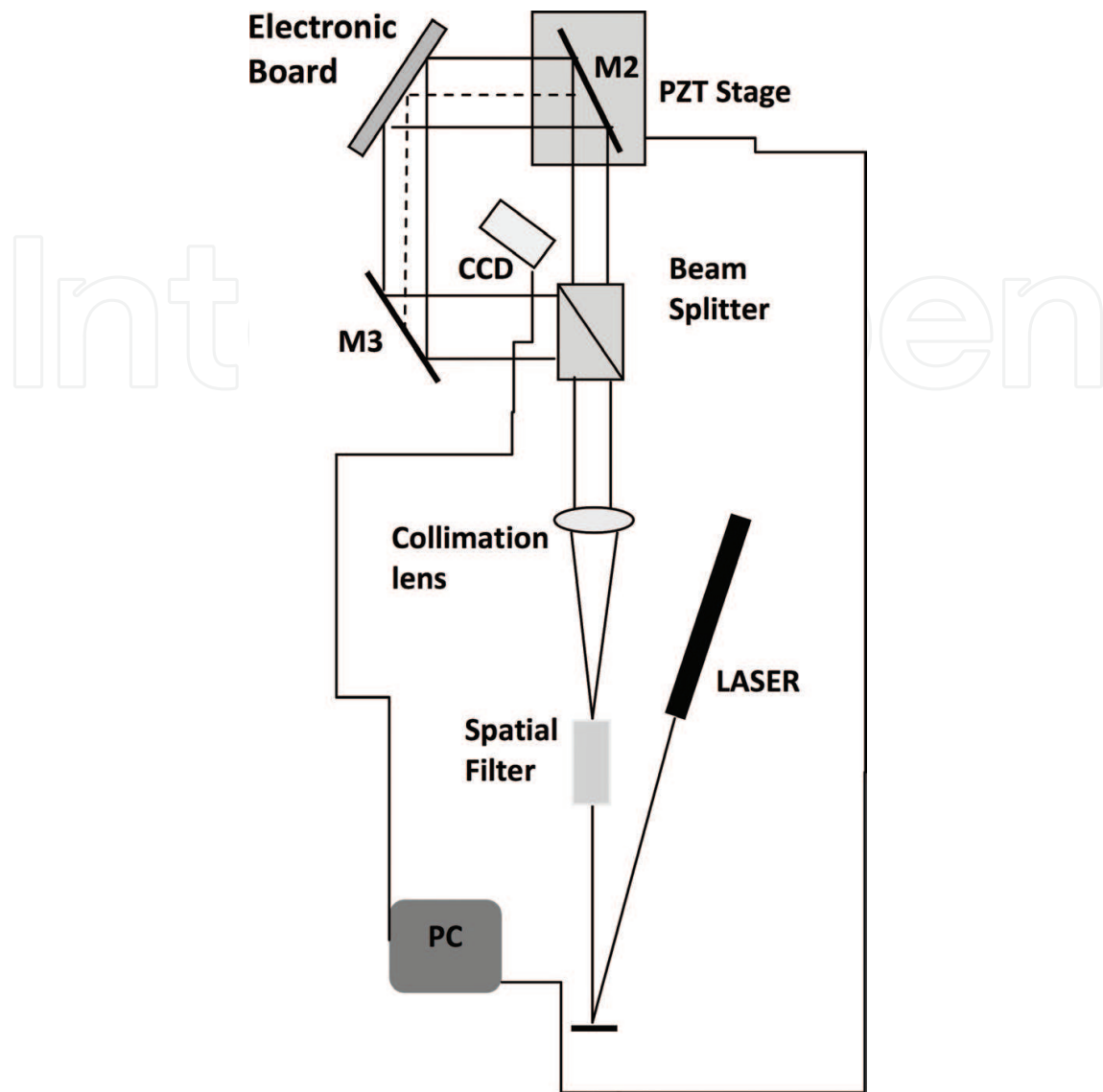


**Figure 1.** Schematic of the implemented phase shifting interferometric speckle setup [12].

The sensitivity  $\lambda/2\sin\theta$  of the optical setup is 447 nm for the given optical-geometrical configuration; this means that points belonging to two adjacent fringes experience a relative displacement along the horizontal in-plane direction of about 0.5  $\mu\text{m}$ . First tests were performed on a NZT605 Darlington transistor mounted on a S9004 electronic board adopted in satellite space application. The board is a DC/DC convertor with a dual output  $\pm 5.7$  V. The indicated transistor was subjected to analysis because it was indicated, by the producer, to be the most critical element in terms of reliability. More in detail, the analyzed component is an NPN Darlington transistor whose gain factor can be up to 10,000 of the input current. It was mounted on a SOT-223 type package (**Figure 2**), which is specifically designed for this kind of application because it guarantees improved performances in terms of thermal dissipation.

The measurement procedure starts by acquiring a set of five reference images, one for each phase step. After this, starting step power was applied to the component, and speckle patterns

were acquired according to a given temporal sequence. These speckle patterns are subtracted one by one from the five reference patterns. When this is done, after proper preprocessing of the images as described above, Eq. (1) is used to calculate wrapped phase, while the spanning tree algorithm implemented in the Fringe Application software is used to obtain the unwrapped phase [14]. Finally, Eq. (2) is used to obtain the displacement maps. The experimental plan was organized in order to understand the thermomechanical behavior of the component both in normal working condition and in the presence of a damage, which can cause malfunctioning of the board. After some preliminary attempts and in accordance with the indications of the producer, this last condition was simulated by powering the board with 29 V instead of the nominal powering voltage of 17 V. This corresponds, at the level of the analyzed component, to an applied voltage 50% higher than the maximum suggested voltage so that this condition simulates working under severe conditions. Having this in mind, two types of tests, that is to say static and fatigue tests, were performed. In the static test, voltage is applied to the board at a given instant time  $t_v$  and the power is kept on for the following 10 minutes. During this phase, speckle patterns are acquired in order to evaluate progression of the  $u$ -displacement field in the heating stage. Ten minutes are enough to reach a stationary state as it was inferred from preliminary investigations. At the end of this stage, the board is powered off, and the following 10 minutes are monitored in order to get information on the evolution of the  $u$ -displacement fields during the cooling phase. The same procedure was finally repeated after 90° rotation of the board in order to measure the  $v$ -displacement field as well, and in such a way, complete description of the in-plane displacement field is obtained. For analyzing the fatigue behavior of the NZT605 component, cyclic powering loading was considered. Two different loading cycles were implemented, and for each of them, two levels of maximum voltage were considered corresponding, as for the static tests, to nominal and anomalous working conditions. A timer was put in series between the power supply and the analyzed board. Timer allows regulation of the on and off time. Experiments were performed under

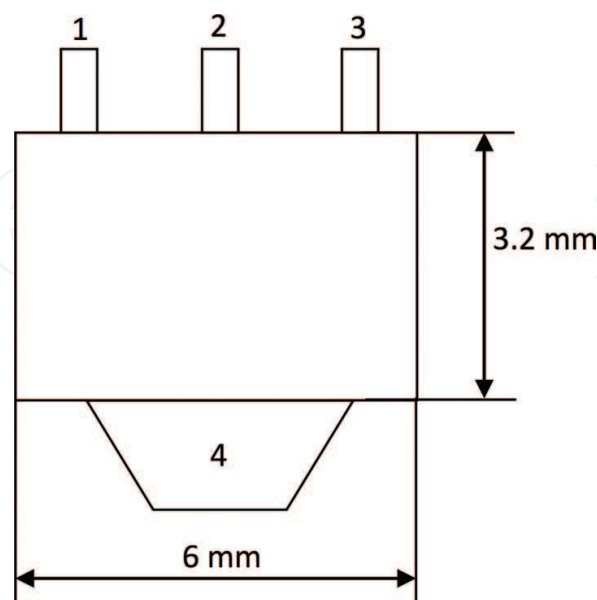


**Figure 2.** Schematic of the SOT-223 packaging.

slow loading conditions, that is to say, with a time duration of each loading cycle  $T_{\text{slow}} = 400$  s and under fast loading conditions, that is to say, with a time duration of each loading cycle  $T_{\text{fast}} = 10$  s. Duty cycle is fixed to 50% for both experimental conditions. The duration of the entire fatigue test was 8 h. It was divided into four steps of 2 h each. At the end of each step, the board is powered off for half an hour, and finally a speckle pattern is acquired. This speckle pattern is subtracted by the five reference patterns recorded at the beginning of the test, and displacement maps are obtained as described for the static test. In this way, it is possible to extract the information on the residual deformation of the component as a consequence of the loading cycles. Five different measurements were performed for each of the loading conditions and repeated for two levels of voltage, 17 and 29 V. As it was stated for the static tests, those two levels are representative of the normal and anomalous working conditions. Finally, a second set of experiments was performed on a LM7818 voltage stabilizer. In this case, the main scope of the analysis was to understand if the PSESPI system could capture difference in the deformation field connected with a bad thermal contact. This was simulated by bad screwing of the component to the board so that the lower part of the body of the component does not adhere perfectly to the board. This is a condition that can appear as a consequence of inappropriate mounting procedure or that can arise as a consequence of warping of the board during exercise. Reference pattern collection and fringe analysis follow the procedure described before. Then, the component is powered to the nominal input power, and 5 s is waited before collecting a speckle pattern. Measurements were repeated five times for each condition.

### 3. Results and discussion

In **Figure 3**, the relative displacement as recorded along the indicated cross section is reported as a function of the test time. In particular (**Figure 3A**), for the case of the  $u$  horizontal displacements, the top and the bottom cross sections are reported, while for the case of the  $v$  vertical displacements (**Figure 3B**), the middle and the bottom cross sections are shown. It is clearly visible how, after 10 minutes of board powering, a three times higher level of  $u$ -displacement is observed in case of anomalous working conditions than normal working conditions ( $3.01 \mu\text{m}$  vs.  $2.73 \mu\text{m}$ ). Analogous conclusions can be done by observing the  $v$ -displacement field.

In fact, when over voltage is applied, a 2.5 times higher displacement in the central section of the component ( $1.46 \mu\text{m}$  vs.  $0.56 \mu\text{m}$ ) can be observed. Deformation field is not homogeneous, and in fact, displacement in the middle of the component is 30% larger than in the bottom part ( $1.46 \mu\text{m}$  vs.  $1.11 \mu\text{m}$ ). This general consideration holds for both normal working and anomalous working conditions. However, it can be observed that those differences are progressively recovered during the cooling state, and at the end of the test, no final residual displacement can be observed. This different behavior during the heating and the cooling stage is interesting to be observed, and it is a simple consequence of the high complexity of the thermo-mechanical problem. To get more understanding, it should be recalled that the SOT-223 package (**Figure 2**) is properly designed to improve heat dissipation capability especially through the pad 4 where high level of current, up to 1.5 A, can flow. However, especially when over voltage is applied, pad 4 is not able to dissipate completely the heat so

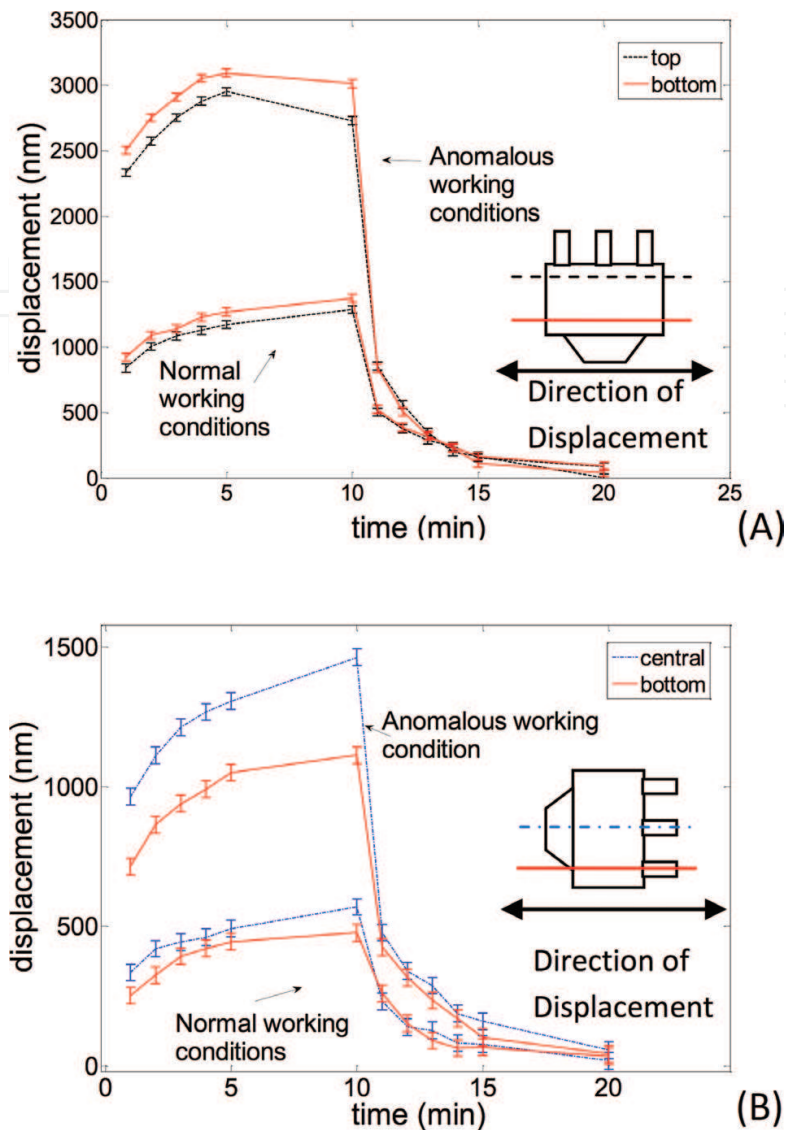


**Figure 3.** Behavior of the displacements recorded along the component during the static tests. (A) horizontal displacements, (B) vertical displacements.

that thermal gradient along the component is higher and this results in a less homogenous displacement field. After powering off the board, no current flows through the collector so that overall thermomechanical behavior rapidly returns to be uniform. This is an important consideration as improving heat flow and dissipation is a critical issue for high power components that can have impact on their reliability and lifetime. Pad 4 is designed to the scope of improving power dissipation but, nevertheless, our measurements that still strain values up to  $500 \cdot 10^{-6} \text{ m/m}$  can be observed.

In **Figure 4**, the results in terms of residual deformation are reported for the 8 hour fatigue tests performed in this study. In particular, the reported data are referred to the region close to the bottom of the component that is to say in the nearby of the pad 4 where both  $u$  displacements and  $v$  displacements are higher. Results for normal working conditions are reported in **Figure 4A**, while results referred to anomalous working conditions are reported in **Figure 4B**.



Statistical dispersion was calculated over five measurements, and it is comparable to that observed for the static tests. It can be observed that if a 10 s cycle duration is considered (i.e., high frequency, fast cycle), no significant residual displacement field can be observed. Final displacement obtained after 8 cycling hours was 50 nm in case of normal working and 200 nm in case of anomalous working that is to say for times higher in this last condition. However, if a 400 s cycle duration is considered (i.e., low frequency, slow cycle), it can be observed that residual u displacements become considerably higher. In fact, a final residual displacement of 202 nm is recorded for 17 V of applied voltage, which increases up to 691 nm when 29 V is applied. In general, by data observation, it can be said that residual deformation accumulates during the test and that it increases about 3.5 times if anomalous working conditions are implemented. If loading histories are compared for the high frequency and low frequency fatigue tests, it should be noted that, in the former case, the board is subjected to a total amount of 2880 cycles, while in the second case, the total number of cycles is 72. When slow cycling is considered, it can be inferred that heat has more time to propagate across the component. Consequently, larger gradients of temperature distribution can build up, and this

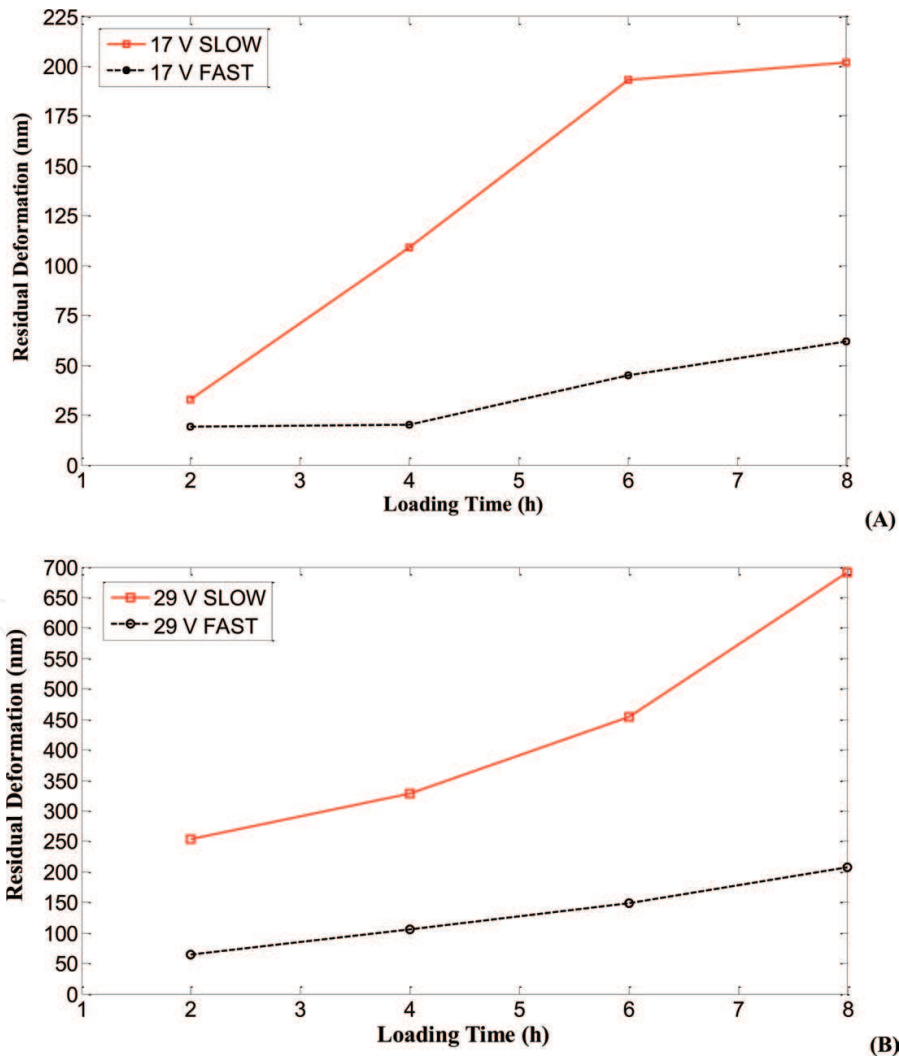
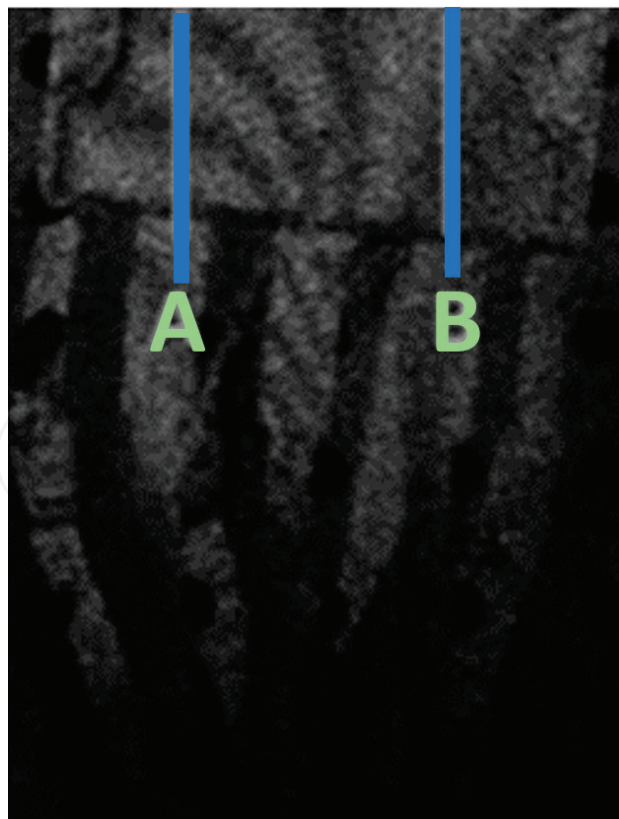


Figure 4. Residual displacements measured at 17 V (A) and 29 V (B) for the cases of slow and fast cycles.

leads to more asymmetry in structural response, which turns, at the end, in larger residual displacements. Of course, the higher the voltage applied to the specimen, more evident is this phenomenon. This leads to another important observation. It should be taken into account that accelerated tests are a powerful tool for reliability assessment [15]; however, the behavior illustrated before shows that proper choice of the voltage must be done in order to have significant findings. Another interesting observation that can be done in relationship with the experimental data is that the increase of residual deformation, when low cycling frequencies are considered, is bigger in anomalous working condition as expected.

**Figures 5** and **6** show the speckle correlation fringes recorded after 5 s of powering of the component [16]. In particular, **Figure 5** shows correlation fringes recorded in case of good thermal contact, while **Figure 6** shows fringe correlation in case of bad thermal contact. It appears soon very evident how fringe pattern changes very much between those two situations. In the case of good thermal contact, it appears evident the inhomogeneous strain distribution connected with the different levels of current flowing in different parts of the components. In the case of bad thermal contact, instead, the displacement field appears to be dominated by the shear component. This can be explained if it is taken into consideration that bad thermal contact configuration was simulated by not perfect adhesion of the lower part of the body of the component to the board. This leads to have two distinct regions in the upper part and in the lower part of the component with very different heat dissipation capability;



**Figure 5.** ESPI correlation fringe pattern recorded on the LM7818 component when good thermal contact between component and board is present.

as a consequence, a temperature gradient which follows the vertical direction arises, and this leads to the appearance of dominant shear deformation. Another interesting observation can be done if the left part and the right part of a positive voltage stabilizer are compared. It should be underlined that input current flows starting from the pin in the left side of the component, while output current flows starting from the pin in the right side. Deformation field appears very different in the two sides mainly as a consequence of different levels of input and output current. This is particularly evident when good thermal contact is realized. Conversely, in the case of bad thermal contact, shear component is dominant and tends to mask this effect. In **Table 1**, the shear strain  $\epsilon_{xy}$  is reported. In particular, this was calculated by following the two lines A and B reported in **Figures 5** and **6**. Section A and B were taken in correspondence of the input and the output pins. It can be easily argued how measurement of  $\epsilon_{xy}$  can be efficiently used to detect the occurrence of bad thermal contact. In this case, in fact,

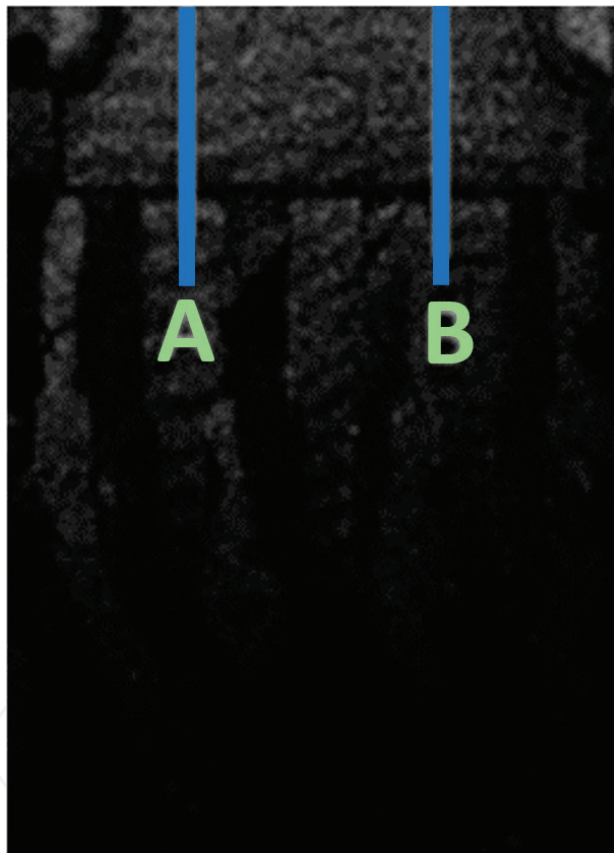


**Figure 6.** ESPI correlation fringe pattern recorded on the LM7818 component when bad thermal contact between component and board is present.

Good thermal contact		Bad thermal contact	
$\epsilon_{xy}$ ( $10^{-6}$ m/m) along A	$\epsilon_{xy}$ ( $10^{-6}$ m/m) along B	$\epsilon_{xy}$ ( $10^{-6}$ m/m) along A	$\epsilon_{xy}$ ( $10^{-6}$ m/m) along B
60	200	850	920

**Table 1.** Shear strain recorded on the LM7818 component in case of good and bad thermal contact.

$\varepsilon_{xy} = 200 \cdot 10^{-6}$  m/m was measured in the nearby of the output pin when good thermal contact is present, while this value rises up to  $\varepsilon_{xy} = 920 \cdot 10^{-6}$  m/m in the case of bad thermal contact.

## 4. Conclusions

In this work, we have reported some results obtained by applying electronic speckle pattern interferometry to measure displacement field of electronic components under different conditions. We have demonstrated how this approach captures the complex deformation field occurring in electronic components. Moreover, the sensitivity of the method is enough to record the small residual deformation field that is accumulated at each powering cycle. This is an important aspect that can have effects in terms of determining reliability of the components under different conditions. Furthermore, it was also found that anomalous conditions as those referred to bad thermal contact can be clearly put in evidence by analyzing the recorded fringe pattern. In this line, this approach can be promising as a diagnostic tool to detect bad mounting conditions. In this specific work, a pixel size of about  $10 \mu\text{m}$  was available, and this was enough to capture details in strain distribution for the analyzed component and to detect, for example, difference in correspondence of different pins. One interesting issue may be how to use ESPI for inspecting thermomechanical behavior of other chips with more complex geometry such as, for example, ASIC, FPGA, and CLPD. This task becomes very challenging especially when the contact between chip and board is realized through ball grid arrays as BGAs include much smaller contact surfaces than the large pad of the SOT-23 package tested in this study. This may entail different selections of sensor type (e.g., to increase spatial resolution) and imaging optics (e.g., to achieve higher magnification). Besides changing properly the field of view and resolution of the sensor, the inherent properties of the speckle field provide immediate information on any irregularities/anomalies in thermal deformation. In particular, local decorrelation or defocusing helps to identify critical regions. Major issues such as, for example, short or open circuits caused in BGAs by thermal stresses can be detected by simply looking at the ESPI pattern structure just by a visual inspection.

In perspective, possibility to miniaturize the system by making use of optical fibers and to use it as a diagnostic tool to test a specific component or a subpart with respect to issues connected with bad contact or damage presence is foreseeable. The large amount of information available from ESPI measurements may certainly help designers to optimize chip geometry and PCB layout. By critically comparing design alternatives, it will be possible to select the best solution that allows risk of failure to be reduced by a great extent.

## Author details

Caterina Casavola, Luciano Lamberti, Vincenzo Moramarco, Giovanni Pappalettera and Carmine Pappalettere\*

\*Address all correspondence to: [carmine.pappalettere@poliba.it](mailto:carmine.pappalettere@poliba.it)

Department of Mechanics, Mathematics and Management, Polytechnic of Bari, Bari, Italy

## References

- [1] Tummala RR. *Fundamentals of Microsystems Packaging*. New York, USA: Mc Graw-Hill; 2001
- [2] Ulrich RK, Brown WD, Ulrich RK. *Advanced Electronic Packaging*. Chichester, UK: Wiley-IEEE Press; 2006
- [3] Jang JW, Suk KL, Paik KW, Lee SB. Measurement and analysis for residual warpage of chip-on-flex (COF) and chip-in-flex (CIF) packages. *IEEE Transactions on Components, Packaging and Manufacturing Technology*. 2012;**2**(6111273):834-840
- [4] Wolter KJ, Oppermann M, Heuer H, Köhler B, Schubert F, Netzelmann U, et al. Micro- and nano-NDE for micro-electronics. In: *Proceedings of the IV Panamerican Conference of NDE*. Buenos Aires (Argentina); 2007
- [5] Sharpe WN, editor. *Handbook of Experimental Solid Mechanics*. New York, USA: Springer; 2008
- [6] Han B, Guo Y. Determination of an effective coefficient of thermal expansion of electronic packaging components: A whole-field approach. *IEEE Transactions on Components, Packaging, and Manufacturing Technology: Part A*. 1996;**19**:240-247
- [7] Nassim K, Joannes L, Cornet A, Dilhaire S, Schaub E, Claeys W. High-resolution interferometry and electronic speckle pattern interferometry applied to the thermomechanical study of a MOS power transistor. *Microelectronics Journal*. 1999;**30**:1125-1128
- [8] Genovese K, Lamberti L, Pappalettere C. A comprehensive ESPI based system for combined measurement of shape and deformation of electronic components. *Optics and Lasers in Engineering*. 2004;**42**:543-562
- [9] Sciammarella CA, Lamberti L, Pappalettere C, Volpicella G, Sciammarella FM. Measurement of deflections experienced by electronic chips during soldering. *Journal of Strain Analysis for Engineering Design*. 2006;**41**:597-608
- [10] Cote KJ, Dadkhah MS. Whole field displacement measurement technique using speckle interferometry. In: *Proceedings of the 51st Conference on Electronic Components and Technology*. Orlando (FL), USA; 2001. pp. 80-84
- [11] Leendertz JA. Interferometric displacement measurement on scattering surface utilizing speckle effect. *Journal of Physics E: Scientific Instruments*. 1970;**3**:214-218
- [12] Casavola C, Lamberti L, Moramarco V, Pappalettera G, Pappalettere C. Experimental analysis of thermo-mechanical behaviour of electronic components with speckle interferometry. *Strain*. 2013;**49**:497-506
- [13] Ghiglia DC, Pritt MD. *Two-Dimensional Phase Unwrapping. Theory, Algorithms and Software*. New York, USA: Wiley Interscience; 1998

- [14] SmartTech Ltd. Fringe Application 2001 Version 1.0, Warsaw (Poland); 2001. [www.smarttech.pl](http://www.smarttech.pl)
- [15] Shiratori M, Qiang Y. Fatigue-strength prediction of microelectronics solder joints under thermal cyclic loading. *IEEE Transactions on Components, Packaging, and Manufacturing Technology: Part A*. 1997;**20**:266-273
- [16] Casavola C, Pappalettera G. Strain field analysis in electronic components by ESPI: Bad thermal contact and damage evaluation. *Journal of Nondestructive Evaluation*. 2018;**37**:11

IntechOpen

